PPPL-1991

PPPL--1991

DE83 010837

KINETIC AND RESISTIVE EFFECTS ON INTERCHANGE INSTABILITIES FOR A CYLINDRICAL MODEL SPHEROMAK

G.W. Hammett and W.M. Tang

Plasma Physics Laboratory, Princeton University

Princeton, New Jersey 08544

April, 1983

ABSTRACT

The stabilizing influence of diamagnetic drift effects on ideal and resistive interchange modes is investigated. A resistive-ballooning-mode equation is derived using a kinetic theory approach and is applied to a cylindrical model spheromak equilibrium. It is found that these kinetic effects can significantly improve the β limits for collisionless interchange stability. For the resistive modes, the diamagnetic drift terms lead to growth rates which scale linearly with resistivity and are considerably reduced in magnitude. However, the resistive interchange growth rates estimated for near-term spheromak parameters remain significant.

DISCLAIMER

This report was prepared as an account of work sponsored by an agency of the United States Government. Neither the United States Government nor any agency thereof, nor any of their employees, makes any warranty, express or implied, or assumes any legal liability or responsibility for the accuracy, completeness, or usefulness of any information, apparatus, product, or process disclosed, or represents that its use would not infringe privately owned rights. Reference herein to any specific commercial product, process, or service by trade name, trademark, manufacturer, or otherwise does not necessarily constitute or imply its endorsement, recommendation, or favoring by the United States Government or any agency thereof. The views and opinions of authors expressed herein do not necessarily state or reflect those of the United States Government or any agency thereof.

DISTRIBUTION OF THIS DOCUMENT IS UNLIMITED

I. INTRODUCTION

It is well-known that the stability requirements for interchange-type modes can strongly influence the maximum value of beta (ratio of plasma pressure to magnetic pressure) achievable in magnetically confined plasmas. The ideal MHD properties of these instabilities for the spheromak (or compact torus) configuration have been calculated in recent work by Jardin.[1] Here it was found that for most cases of interest a cylindrical model spheromak equilibrium provides a good approximation to the actual toroidal system. In the present paper we will consider the influence of kinetic and resistive effects on radially-localized interchange modes for this cylindrical configuration.

The spheromak configuration is a scheme for confining a plasma in a torus without external magnetic field coils linking the torus. The plasma carries its own poloidal and toroidal currents to generate its internal toroidal and poloidal magnetic fields. Consequently, there is no toroidal field outside the spheromak and the safety factor q is zero at the edge of the plasma. The cylindrical model for the spheromak can be conceptually viewed in the same way as for the tokamak. The torus (of major and minor radii R and a) is cut at one toroidal location and straightened into a cylinder of radius a and length $2\pi R$. A simple model for q in a spheromak is $q(r) = q_o\ (1-r^2/a^2)$. The reversed-field-pinch (RFP) is closely related to the spheromak. It has a much larger aspect ratio (R/a) and has external toroidal field coils which reverse the toroidal field at the edge of the plasma. A simple q-profile for the RFP is $q(r) = q_o(1-r^2/b^2)$, where $b < a$ so that q changes sign. Note that dq/dr for a spheromak has the opposite sign from dq/dr for a tokamak.

One might at first suspect that using a cylindrical model of the small aspect ratio spheromak $(R/a \sim 2)$ would not be appropriate since toroidal effects are known to be important for many modes. However, this simple model proves to be quite adequate when dealing with interchange type instabilities. This is due to the fact that since $q < 1$ in spheromaks, the average field curvature is already unfavorable.[2] Hence, in contrast to tokamaks (where q is maintained above one over most of the discharge), the poloidal variation of field curvature associated with toroidal effects will introduce generally negligible corrections to interchange mode stability properties in spheromaks.

In previous investigations of resistive and diamagnetic drift effects on interchange instabilities, the general approach has been to use the ideal MHD equations together with a modified Ohm's law equation including the resistive and Hall terms.[2,3] This leads to a fourth-order radial eigenmode equation governing both resistive interchange and tearing modes. Coppi[3] has noted that to study just the resistive interchanges it is convenient to carry out the analysis in k-space (with k being the radial wave number). The resultant eigenmode equation is a second order differential equation which has the same structure as the one derived in Sec. II from a kinetic theory approach [Eq. (2.22)]. Working with this form, we analyze the kinetic stabilization of ideal interchange modes in Sec. III and illustrate the improved beta limits relative to the MHD results of Ref. 1. In Sec. IV we go on to calculate the diamagnetic drift effects on resistive interchange modes and estimate their growth rates for representative spheromak parameters. Finally, the results from our studies are briefly summarized and discussed in Sec. V.

II. THE KINETIC-RESISTIVE-BALLOONING EQUATION

A systematic procedure for calculating the influence of kinetic effects on collisionless ballooning modes for general geometry has been presented in earlier work.[4] The present derivation of the resistive ballooning mode equation follows this procedure with the important exception that a model Krook operator has been added to account for collisional dissipation.

Ballooning modes are characterized by short perpendicular and long parallel wavelengths, $k_\perp \gg k_\parallel$, so that an eikonal representation for all perturbed quantities is appropriate, i.e.,

$$\begin{pmatrix} f \\ \phi \\ \vec{A} \end{pmatrix} = \begin{pmatrix} \hat{f} \\ \hat{\phi} \\ \hat{\vec{A}} \end{pmatrix} e^{iS} \tag{2.1}$$

where $\nabla S = \vec{k}_\perp$ accounts for the rapid cross-field variations and $\hat{f}$, $\hat{\phi}$, and $\hat{\vec{A}}$ account for the slow variations along the field line. Here f is the perturbed particle distribution function, and ϕ and $\vec{A}$ are the perturbed electric potential and magnetic vector potential.

In order to satisfy $\hat{n} \cdot \vec{k}_\perp = 0$ everywhere ($\hat{n} \equiv \vec{B}/|\vec{B}|$ is direction of the magnetic field), $\vec{k}_\perp$ must vary along the field line. Specifically, since

$$\nabla (\hat{n} \cdot \vec{k}_\perp) = \hat{n} \cdot \nabla\vec{k}_\perp + (\nabla\hat{n}) \cdot \vec{k}_\perp \equiv 0 \quad , \tag{2.2}$$

we can write

$$\frac{\partial \vec{k}_\perp}{\partial \ell} = \hat{n} \cdot \nabla \vec{k}_\perp = -(\nabla\hat{n}) \cdot \vec{k}_\perp \tag{2.3}$$

where ℓ is the distance along the field line. In cylindrical (r, θ, z) geometry, the solution to Eq. (2.3) is

$$\vec{k}_\perp = k_z\left(-\frac{B_z}{B}\frac{q'}{q}\,\ell\hat{r} - \frac{B_z}{B_\theta}\,\hat{\theta} + \hat{z}\right) \tag{2.4}$$

Here k_z is a constant, B_z and B_θ are components of the magnetic field in the axial and azimuthal directions, $q \equiv rB_z/RB_\theta$ is the safety factor, and $q' = dq/dr$. Note that the radial component of $\vec{k}_\perp$ varies along the field line because of shear ($q' \neq 0$).

The slowly varying amplitudes $\hat{f}$, $\hat{\phi}$, and $\hat{\vec{A}}$ are related to each other by the gyrokinetic equation, the quasineutrality condition, and Ampere's law. In this paper we will restrict our attention to modes with $k_\perp \rho_i << 1$ and take the equilibrium distribution function to be Maxwellian, F_m. With these assumptions, the gyrokinetic equation including a Krook collision operator is[4-6]

$$v_\parallel \frac{\partial \hat{h}}{\partial \ell} - i(\omega - \vec{k}_\perp \cdot \vec{v}_d)\hat{h} = -\nu\left(\hat{h} - \frac{F_m}{n_o}\int d^3v\hat{h}\right) - iF_m(\omega - \omega_*)$$
$$\times \left\{J_o\left(\frac{e\hat{\phi}}{T} - \frac{v_\parallel}{c}\frac{e\hat{A}_\parallel}{T}\right) + \frac{mv_\perp^2}{2T}\frac{\delta\hat{B}_\parallel}{B}\right\} . \tag{2.5}$$

Quasineutrality and the two relevant components of Ampere's law are

$$\hat{\phi}\,\Sigma\,\frac{n_o e^2}{T} = \Sigma\, e \int d^3v\hat{h}J_o \quad , \tag{2.6}$$

$$k_\perp^2\hat{A}_\parallel = \frac{4\pi}{c}\,\Sigma\, e\int d^3v\hat{h}v_\parallel J_o \quad , \tag{2.7}$$

and

$$\delta\hat{B}_\parallel = -4\pi\;\Sigma\int d^3v\hat{h}\,\frac{mv_\perp^2}{2B} \quad . \tag{2.8}$$

In these equations, $\hat{h}(E, \mu, \sigma, \ell)$ is the nonadiabatic part of the perturbed distribution function, where the independent variables are the energy $E = v_\parallel^2/2 + \mu B$, the magnetic moment $\mu = v_\perp^2/2B$, and $\sigma = \text{sign}(v_\parallel)$. $v_\parallel$ and $v_\perp$ are the parallel and perpendicular components of the particle velocity, and $\vec{v}_d$ is the guiding center drift defined as

$$\vec{v}_d = \frac{1}{\Omega}\,\vec{n} \times (\mu\nabla B + v_\parallel^2\hat{n}\cdot\nabla\hat{n}) \qquad (2.9)$$

where $\Omega \equiv eB/mc$ is the gyro frequency; e, m, n_o, and T are species charge, mass, density, and temperature; Σ means summation over species; and $\int d^3v$ is integration over velocity space. The mode frequency is $\omega = \omega_r + i\gamma$, where γ is the growth rate, and $\gamma > 0$ for instability. The collision frequency is represented by ν, and the diamagnetic drift frequency is defined as

$$\omega_* = \frac{cT}{eB}\ \vec{k}_\perp\cdot(\hat{n} \times \nabla \ln n_o) \ . \qquad (2.10)$$

(We have assumed $\nabla T = 0$ consistent with the use of a simple form of the Krook operator which does not conserve energy.) $\hat{A}_\parallel$ and $\delta\hat{B}_\parallel$ are the parallel components of the perturbed vector potential and the perturbed magnetic field. Finally, the Bessel functions in Eqs. (2.6) and (2.7) are expanded in the small $k_\perp\rho_i$ limit, i.e., $J_o = 1 - (k_\perp^2 v_\perp^2/4\Omega^2)$ for ions, while $J_o = 1$ for electrons.

We derive the resistive ballooning equation in the regime where ions are fluidlike and collisionless while electrons are adiabatic and collisional. The frequency ordering for this regime is

$$\nu_i \ll k_\parallel v_{ti} \ll \vec{k}_\perp \cdot \vec{v}_d \lesssim \omega \sim \omega_* \ll k_\parallel v_{te} \ll \nu_e \ .$$

Here v_t is the thermal speed and subscripts i and e denote ions and electrons. Drift waves are ordered out of the problem by setting $E_\parallel = 0$ to lowest order. This implies $k_\parallel \hat{\phi} \sim (\omega/c)\hat{A}_\parallel$ and $(v_t/c)(e\hat{A}_\parallel/T) \gg e\hat{\phi}/T$ for electrons while the opposite inequality holds for ions.

To calculate the electron response we first introduce the small parameter $\varepsilon \sim (\omega/k_\parallel v_{te}) \sim (k_\parallel v_{te}/\nu_e) \ll 1$, and expand the distribution function $\hat{h} = \hat{h}_o + \varepsilon\hat{h}_1 + \varepsilon^2\hat{h}_2 + \ldots$. Eq. (2.5) to lowest order in ε yields

$$\hat{h}_o = \frac{F_m}{n_o} \int d^3v\hat{h}_o = \frac{F_m}{n_o} n_{e1} \ . \tag{2.11}$$

It is necessary to go to higher order to determine n_{e1}. The first and second order equations are

$$v_\parallel \frac{\partial \hat{h}_o}{\partial \ell} = -\nu\left(\hat{h}_1 - \frac{F_m}{n_o} \int d^3v\hat{h}_1\right) + i\, F_m(\omega - \omega_*)\frac{v_\parallel}{c}\frac{e\hat{A}_\parallel}{T} \tag{2.12}$$

$$v_\parallel \frac{\partial \hat{h}_1}{\partial \ell} - i(\omega - \vec{k}_\perp \cdot \vec{v}_d)\hat{h}_o = -\nu\left(\hat{h}_2 - \frac{F_m}{n_o}\int d^3v\hat{h}_2\right) - i\, F_m(\omega - \omega_*)$$

$$\times \left\{\frac{e\hat{\phi}}{T} + \frac{mv_\perp^2}{2T}\frac{\delta\hat{B}_\parallel}{B}\right\} \ . \tag{2.13}$$

These two first-order differential equations can be combined into a single second-order differential equation after operating on Eq. (2.12) with $\int d^3v\, v_\parallel$ and on Eq. (2.13) with $\int d^3v$. The resultant single equation becomes

$$\frac{\partial}{\partial \ell}\left[\frac{k_\perp^2}{1+i\eta c^2k_\perp^2/4\pi(\omega-\omega_{*e})}\frac{\partial n_{e1}}{d\ell}\right] = \frac{4\pi n_o e^2}{T_e c^2}(\omega-\omega_{*e})\Big[-n_{e1}(\omega-\omega_{de})$$

$$+ n_o(\omega-\omega_{*e})\Big(-\frac{|e|\hat{\phi}}{T_e} + \frac{\delta\hat{B}_\parallel}{B}\Big)\Big] \qquad (2.14)$$

where

$$\eta = \frac{m_e \nu_e}{n_o e^2} \quad ,$$

$$\omega_B = \left(\frac{T}{m\Omega B}\right)\vec{k}_\perp \cdot (\hat{n} \times \nabla B) \quad ,$$

$$\omega_\kappa = \left(\frac{T}{m\Omega}\right)\vec{k}_\perp \cdot [\hat{n}\times(\hat{n}\cdot\nabla\hat{n})] \quad ,$$

and

$$\omega_d = \omega_B + \omega_\kappa = \int d^3v\, \frac{F_m}{n_o}(\vec{k}_\perp \cdot \vec{v}_d) \quad . \qquad (2.15)$$

In Eq. (2.14), we have made use of the fact that the ion contribution to the parallel current is negligible so that Eq. (2.7) becomes

$$\hat{A}_\parallel = -\frac{4\pi}{ck_\perp^2}|e| \int d^3v\, v_\parallel\, \hat{h}_{1e} \quad . \qquad (2.16)$$

Now consider the ion response, which to lowest order is

$$\hat{h}_i = F_m\left(\frac{\omega-\omega_{*i}}{\omega-\vec{k}_\perp\cdot\vec{v}_{di}}\right)\left\{J_o\frac{|e|\hat{\phi}}{T_i} + \frac{m_i v_\perp^2}{2\,T_i}\frac{\delta\hat{B}_\parallel}{B}\right\} \quad . \qquad (2.17)$$

In order to take velocity moments of $\hat{h}_i$ easily, we assume $\omega_{di} < \omega$ and expand

$$(\omega-\vec{k}_\perp\cdot\vec{v}_{di})^{-1} = \frac{1}{\omega}\left(1 + \frac{\vec{k}_\perp\cdot\vec{v}_{di}}{\omega}\right) .$$

In addition to the moment given by Eq. (2.15), quasineutrality and Ampere's law make use of

$$\int d^3v\ F_m \frac{\vec{k}_\perp\cdot\vec{v}_{di}}{\omega}\frac{m_i v_\perp^2}{2T_i} = n_o \frac{\omega_{di} + \omega_{Bi}}{\omega} \qquad . \qquad (2.18)$$

Further simplification results from noting that $\delta\hat{B}_\parallel/B \sim \beta e\hat{\phi}/T_i$, and assuming $\beta << 1$. After some tedious but straightforward algebra, Eqs. (2.6) and (2.8) yield to first order in β, ω_{di}/ω, and $k_\perp^2\rho_i^2$

$$-\frac{|e|\hat{\phi}}{T_e} + \frac{\delta\hat{B}_\parallel}{B} \approx \frac{n_{e1}}{n_o}\left(\frac{\omega}{\omega-\omega_{*e}}\right)\Big[1 - k_\perp^2 \frac{T_e}{M_i\Omega_i^2}\left(\frac{\omega-\omega_{*i}}{\omega-\omega_{*e}}\right)$$

$$- \frac{1}{(\omega-\omega_{*e})\omega}\{(\omega - \omega_{*i})\omega_{de} + (\omega_{*i} - \omega_{*e})(\omega_{Be} - \omega_{\kappa e})\}\Big] \qquad . \qquad (2.19)$$

Combining this result with Eq. (2.14) produces the kinetic-resistive-ballooning equation

$$\frac{\partial}{\partial \ell}\left[\frac{k_\perp^2}{1+i\eta c^2 k_\perp^2/4\pi(\omega-\omega_{*e})}\frac{\partial n_{e1}}{\partial \ell}\right] + \frac{1}{v_A^2}\Big[k_\perp^2\ \omega(\omega - \omega_{*i})$$

$$+ \frac{2M_i\Omega_i^2}{T_i}\ \omega_{\kappa i}\ \omega_{*p}\Big]\, n_{e1} = 0 \qquad (2.20)$$

with

$$v_A^2 = \frac{B^2}{4\pi n_o M_i} \ , \qquad \omega_{*p} = \omega_{*i} - \omega_{*e} = \frac{2}{\beta_i}(\omega_{\kappa i} - \omega_{Bi}) \ , \tag{2.21}$$

and

$$\beta_i = \frac{n_o T_i}{B^2/8\pi} \ .$$

Up to this point, no assumptions about the magnetic geometry have been made. In the limit where η , ω_{*i}, and ω_{*e} are all zero, while ω_{*p} is retained, Eq. (2.20) reduces to the ideal ballooning mode equation.[7]

In cylindrical geometry, $\vec{k}_\perp(\ell)$ is given by Eq. (2.4), and Eq. (2.20) reduces to the kinetic-resistive-interchange equation, which in dimensionless form is

$$\frac{\partial}{\partial x}\left[\frac{1+x^2}{1+i\gamma_R(1+x^2)/(\omega-\omega_{*e})}\frac{\partial n_{e1}}{\partial x}\right] + \left[(1+x^2)\frac{\omega(\omega-\omega_{*i})}{\gamma_A^2} + D\right]n_{e1} = 0 \ . \tag{2.22}$$

Here, x is the distance along the field line normalized to the shear length s^{-1}, $x = s\ell$, $s = (q'/q)(B_\theta B_z/B^2)$, $k_\perp^2 = k_o^2\,(1 + x^2)$, $k_o^2 = (m^2/r^2) + (n^2/R^2)$, and $n = m/q$. The poloidal and toroidal mode numbers are m and n, R is the major radius, the characteristic Alfvén and resistive frequencies are $\gamma_A = sv_A$ and $\gamma_R = (\eta c^2/4\pi)k_o^2$. The variable D is known as Suydam's parameter. Ideal MHD interchange modes are unstable if D > 1/4 with $D = -(8\pi B_\theta^2/s^2 r B^4) \times (dp/dr)$ and $p = n_o\,(T_e + T_i)$. Equation (2.22) is of the form

$$\frac{\partial}{\partial x}\left[A(x)\frac{\partial\psi}{\partial x}\right] + B(x)\,\psi = 0 \ .$$

Substituting $\psi = A^{-1/2}\,\phi$ eliminates the first derivative term, yielding

$$\frac{\partial^2\phi}{\partial x^2} + Q(x,\omega)\;\phi = 0 \tag{2.23}$$

$$Q(x,\omega) = \left(E + \frac{D}{1+x^2}\right)\left[1 + i\epsilon\left(1 + x^2\right)\right] - \frac{1+i\epsilon(1+x^2)(1-3x^2)}{(1+x^2)^2\,[1+i\epsilon(1+x^2)]^2}$$

$$E = \frac{\omega(\omega-\omega_{*i})}{\gamma_A^2}$$

$$\epsilon = \frac{\gamma_R}{\omega-\omega_{*e}}$$

The eigenfrequency ω must be chosen to satisfy the boundary conditions $\phi \to 0$ as $x \to \pm\infty$. We have used a shooting code to solve numerically Eq. (2.23) and to study the dependence of ω on the parameters D, γ_A, γ_R, ω_{*i}, and ω_{*e}. These results are discussed in the next two sections.

III. KINETIC EFFECTS ON IDEAL INTERCHANGE MODES

In the absence of collisions Q becomes real and Eq. (2.23) can be written in a form reminiscent of the Schrödinger equation of quantum mechanics,[8] i.e.,

$$\frac{\partial^2\phi}{\partial x^2} + \left(E - V(x)\right)\phi = 0 \tag{3.1}$$

$$E = \frac{(\omega-\omega_{*i})^2}{\gamma_A^2}$$

$$V(x) = \frac{1}{(1+x^2)^2} - \frac{D}{1+x^2} + \frac{1}{4}\,\frac{\omega_{*i}^2}{\gamma_A^2}\;.$$

An instability exists only if the energy E is negative. In the MHD limit $\omega_{*i} = 0$, negative energy requires a potential well deep enough (D large enough) so that a bound state exists. Asymptotic analysis of Eq. (3.1) between the turning points of the well, $D/E \gg x^2 \gg 1/D > 1$, leads to the requirement that $D < 1/4$ for stability (Suydam's criterion).

When ω_{*i} is not zero, Suydam's criterion is relaxed. The $\omega_{*i}{}^2$ term in V is positive and pushes the energy upward toward stability so that the well must be even deeper before the mode is unstable. The growth rate $\gamma^2 = -\gamma_A^2 E$ can be expressed as

$$\gamma^2 = \gamma_{MHD}^2 (D) - \frac{1}{4} \omega_{*i}^2 \tag{3.2}$$

where γ_{MHD} is the growth rate found by solving Eq. (3.1) in the MHD limit $\omega_{*i} = 0$. Kulsrud[9,10] found an asymptotic approximation for γ_{MHD} (D) which is plotted in Fig. 1. Our results with the numerical shooting code are in good agreement with the analytic solution. A typical numerical solution of Eq. (2.22) in the collisionless limit is plotted in Fig. 2. As D falls, the mode becomes more extended along the field line.

The stability criterion is now $|\omega_{*i}|/2 > \gamma_{MHD}$ (D). Because γ_{MHD} exponentially falls very rapidly as D approaches 1/4, even small values of ω_{*i} allow significant relaxation of Suydam's criterion. Since $\omega_{*i} \propto dp/dr \propto D$, it is convenient to divide the stability criterion by D to get

$$\frac{n}{4} R \left| \frac{dq}{dr} \right| \frac{c}{r\, \omega_{pi}} \frac{[q^2+(r/R)^2]^{1/2}}{1 + T_e/T_i} > \frac{\gamma_{MHD} (D)}{D\, \gamma_A} \quad . \tag{3.3}$$

$\omega_{pi} = (4\pi n_e e^2/m_i)^{1/2}$ is the ion plasma frequency.

Equation (3.3) is a local stability criterion and gives the maximum allowable D at every point in the minor radius r. A simple example will illustrate the significant relaxation of Suydam's criterion. We consider here the parameters expected for the S-1 spheromak: $n_e = 10^{14}\ cm^{-3}$, R = 45 cm, a = 25 cm, $T_e = T_i$, and parametrize q by $q(r) = (a/R)\ (1-r^2/a^2)$. From Eq. (3.3) and Fig. 1 we find that the plasma is stable against all interchange modes with $n \geq 1$ as long as $D < 0.375$ everywhere. Near the edge of the plasma, where the density is lower, the critical value for D is even larger than 0.375. The β limits implied by Eq. (3.3) are therefore at least 50% higher than the limit given by Suydam's criterion.

The improvement in β made possible by ω_* effects is illustrated by Fig. 3 which is adapted from Ref. 1. Here we plot β_θ versus q_o, where q is assumed of the form $q(r) = q_o\ (1 - r^2/a^2)$, and β_θ is defined by

$$\beta_\theta = \frac{\int_o^a dr\ r^2 p}{\int_o^a dr\ r^2\ B_\theta^2/8\pi} \quad .$$

The β_θ limit implied by Suydam's condition is given by the broken curve. If diamagnetic drift effects allow D to be 0.375, then the β_θ limit is given by the higher solid curve. Also plotted in Fig. 3 is the β_θ limit found by Jardin[1] for stability against finite-n modes with a conducting wall at the edge of the plasma. An important area for future research would be to assess the influence of ω_* effects on these modes. Specifically, it would be interesting to determine whether the β limits for stability against finite-n modes would improve as significantly as they do for high-n interchange modes.

IV. KINETIC EFFECTS ON RESISTIVE INTERCHANGE MODES

Although magnetic shear can stabilize the ideal (collisionless) interchange modes, it cannot provide stability for resistive interchange modes. Resistivity allows field lines to slip through one another and leads to instability whenever D > 0.

An illustrative solution of the full resistive interchange equation, Eq. (2.23), is plotted in Fig. 4. The parameter values taken are $\gamma_A = 3.5 \times 10^6$ sec^{-1}, $\gamma_R = 7.5 \times 10^3$ sec^{-1}, $\omega_{*e} = -\omega_{*i} = 8.5 \times 10^4$ sec^{-1}, and D = 0.0755. The growth rate was found to be 5.7×10^4 sec^{-1} while the real part of the frequency was much smaller, $\omega_r = 7.6 \times 10^2$ sec^{-1}. These values are typical for an m=10 mode localized near r=a/2 in a spheromak plasma with parameters given in line 1 of Table I. For smaller values of resistivity, the eigenmode becomes more extended along the field line.

The growth rate depends on five independent variables. This dependence is conceptually simplified by considering Eq. (2.23) as an eigenvalue problem for E, while D and ε are treated as independent parameters. We numerically solved Eq. (2.23) to find E for many different values of D and ε (Figs. 5 and 6). In the limit of small $|\varepsilon|$ and D (i.e., small resistivity and small pressure gradient), the numerical results are simply summarized by $E = -i\varepsilon D^2$, which leads to the dispersion relation

$$\omega(\omega - \omega_{*i})(\omega - \omega_{*e}) = i\gamma_R \gamma_A^2 D^2 . \tag{4.1}$$

This cubic equation has one unstable root. There are other modes with growth rates not given by Eq. (4.1). However, this appears to be the most unstable mode.

The solution of Eq. (4.1) is plotted in Fig. 7 as a function of k_o ($\omega_* \propto k_o$, $\gamma_R \propto k_o^2$, $\omega_{*e} = -\omega_{*i}$). In the limit $\omega_* \ll \omega$, we recover the well-known resistive MHD growth rate

$$\gamma_{MHD} = [\gamma_R \gamma_A^2 D^2]^{1/3} . \tag{4.2}$$

In the opposite limit $\omega_* \gg \omega$, the growth rate is greatly reduced and scales linearly with γ_R

$$\gamma_{kin} = \frac{\gamma_R \gamma_A^2 D^2}{\omega_{*i}^2} = \frac{m_e}{m_i} \nu_e \frac{4(1+T_e/T_i)^2}{(Rdq/dr)^2} \quad . \tag{4.3}$$

Notice that the true growth rate γ is always less than γ_{MHD} and γ_{kin}, and that γ_{kin} is independent of k_o. In a hot plasma γ_{kin} is usually the appropriate approximation for γ, and a convenient numerical formula is given by

$$\gamma < \gamma_{kin} = \left(\frac{n_e}{10^{14}\ cm^{-3}}\right)\left(\frac{T_e}{1\ keV}\right)^{-3/2}\left(R\ \frac{dq}{dr}\right)^{-2}\ 10^3\ sec^{-1}\ . \tag{4.4}$$

Table I compares order-of-magnitude growth rates for various plasma parameters. In evaluating Eqs. (4.1) — (4.3) we have set $r = a/2$, $dp/dr = p/a$, $dq/dr = q/a$, $n = 1/q$, and $m = 1$. The growth rates for higher m modes will be larger than $\gamma(m = 1)$ and smaller than γ_{kin}. For parameters appropriate to spheromaks in the near future, the growth rates of the resistive interchange modes appear to be significant. The ω_* corrections can be important for high mode numbers. Parameters achieved in the reverse field pinch ZT-40M are used in the second line of Table I.[11] The predicted linear growth rates are significant compared to the lifetime of the plasma, indicating that some nonlinear mechanism is probably preventing the growth of the these modes above a certain amplitude. The last line is for a conceptual spheromak D-T reactor[12] and indicates that the ω_* effects can significantly reduce the growth rate in a hot plasma even for relatively small mode numbers.

The kinetic-resistive-interchange equation, derived in the ordering $k_\perp v_{ti} \ll \omega \ll k_\parallel v_{te} \ll \nu_{ei}$, always predicts instability when the pressure gradient and resistivity are non-zero. Finn et al.[2] arrive at the same prediction of instability using the fluid equations in the limit $\Gamma = 0$, where Γ is the ratio of specific heats. However, for realistic Γ (~ 1), they find that the associated coupling to the acoustic branch, along with ω_* effects in the generalized Ohm's Law, can lead to stability ($\gamma < 0$) for sufficiently small resistivity. Such effects could also be analyzed with the kinetic approach by relaxing the $k_\parallel v_{ti} \ll \omega$ assumption.

V. CONCLUSIONS

In the present paper it has been demonstrated that by employing a ballooning-type representation for the perturbations of interest, the drift-kinetic formalism leads to the same basic eigenmode equation governing localized interchange modes as that obtained by conventional MHD procedures with a modified Ohm's law. For the cylindrical model spheromak equilibrium, solutions to this equation indicate that in the ideal (collisionless) limit, the usual Suydam constraint, $D < 1/4$, can be substantially relaxed when ω_* effects are taken into account. Specifically, for representative parameters, the critical β_θ for ideal interchange stability can be enhanced by 50%. The effects of the diamagnetic drifts on finite-n mode remains to be worked out.

It is well-known that resistivity can destabilize interchange modes in the $D < 1/4$ regime. Here it is found that the kinetic effects can substantially reduce the magnitude of these growth rates and produce a transition in scaling from $\eta^{1/3}$ to η. Further refinement of the kinetic approach to include coupling to sound waves may completely stabilize the resistive interchange modes at high enough temperatures.[2] Nevertheless, growth rates calculated from parameters typical of the S-1 spheromak indicate that resistive interchange modes can remain significant. This points to the need for a nonlinear analysis estimating their saturation and the associated enhanced transport in order to assess the importance of these resistive instabilities.

ACKNOWLEDGMENTS

We wish to thank R. B. White for furnishing his WKB shooting code and L. Chen for helpful discussions. This work was supported by the U.S. Department of Energy Contract NO. DE-AC02-76-CHO-3073.

REFERENCES

[1]S. C. Jardin, Nucl. Fusion 22, 629 (1982).

[2]J. M. Finn, W. M. Manheimer, and T. M. Antonsen, Jr., NRL Memorandum Report 4783, (April 1982).

[3]B. Coppi, Phys. Fluids 7, 1501 (1964).

[4]W. M. Tang, J. W. Connor, and R. J. Hastie, Nucl. Fusion 20, 1439 (1980).

[5]P. J. Catto, W. M. Tang, and D. E. Baldwin, Plasma Phys. 23, 639 (1981).

[6]T. M. Antonsen, Jr., and B. Lane, Phys. Fluids 23, 1205 (1980).

[7]J. W. Connor, R. J. Hastie, J. B. Taylor, Proc. R. Soc. London Ser. A: 365, 1 (1979).

[8]J. W. Connor, W. M. Tang, and J. B. Taylor, "Influence of Gyroradius and Dissipation on the Alfvén Wave Continuum," Phys. Fluids (in press).

[9]R. M. Kulsrud, Phys. Fluids 6, 904 (1963).

[10]T. E. Stringer, Nucl. Fusion 15, 125 (1975).

[11]ZT-40 Team, in Proc. of the Ninth Int.'l Conf. on Plasma Physics and Controlled Fusion Research, Baltimore, MD, 1982, IAEA-CN-41/H-2-1.

[12]M. Katurai, M. Yamada, Nucl. Fusion 22, 1407 (1982).

TABLE 1

q	a (cm)	R (cm)	T_e (ev)	n_e (cm^{-3})	B (K gauss)	$\gamma(m=1)$ (sec^{-1})	$\gamma_{MHD}(m=1)$ (sec^{-1})	γ_{kin} (sec^{-1})
0.25	25	50	150	1.0×10^{14}	8.0	1.6×10^{4}	1.7×10^{4}	7.1×10^{4}
0.09	20	114	200	1.5×10^{13}	2.5	7.1×10^{3}	2.8×10^{4}	7.2×10^{3}
0.25	200	400	15000	1.7×10^{14}	50.0	1.6×10^{2}	9.0×10^{2}	1.6×10^{2}

FIGURE CAPTIONS

FIG. 1. Comparison of numerical and analytic calculations of the growth rate given by ideal MHD.

FIG. 2. The eigenmode ϕ and the potential $-Q = V-E$ for an ideal MHD interchange mode.

FIG. 3. β_θ limits for stability. The broken curve is Suydam's criterion. The solid curve assumes that ω_* effects relaxes Suydam's condition to $D < 0.375$. The dashed curve is for finite-n modes with a conducting shell at the plasma edge (taken from Ref. 1).

FIG. 4. The eigenmode ϕ and the potential $-Q$ for a resistive kinetic interchange mode.

FIG. 5. Numerical results showing the relationship between E and ε for fixed D.

FIG. 6. Numerical results showing the relationship between E/ε and D for small $|\varepsilon|$.

FIG. 7. Scaling of the growth rate with k_o illustrating the MHD limit and the kinetic limit.

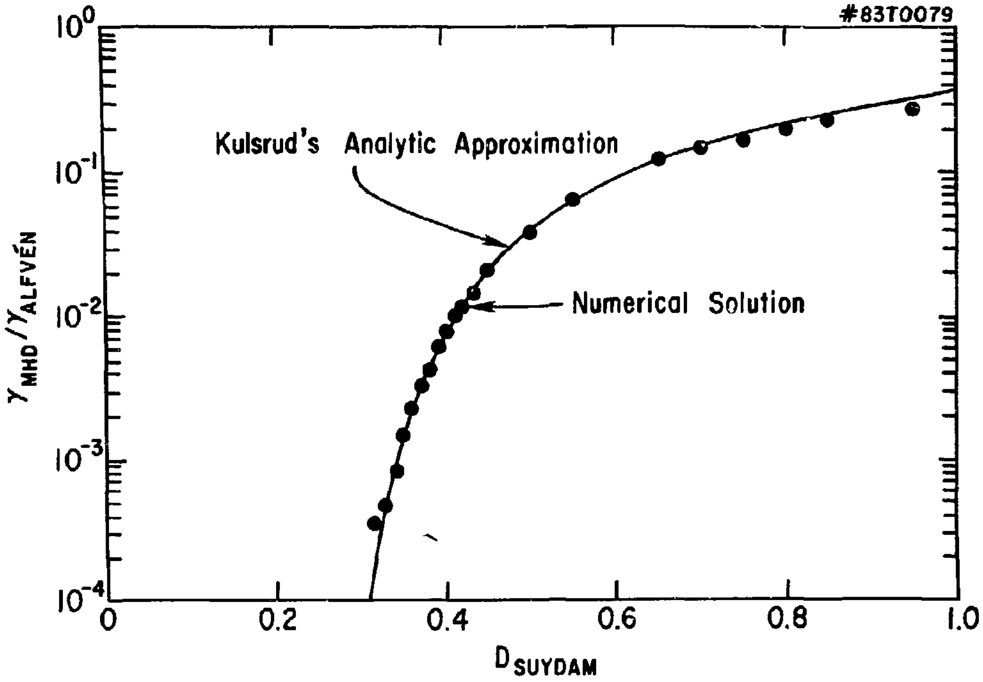
#83T0079
Kulsrud's Analytic Approximation
Numerical Solution
10^0
10^{-1}
10^{-2}
10^{-3}
10^{-4}
$\gamma_{MHD}/\gamma_{ALFVÉN}$
0
0.2
0.4
0.6
0.8
1.0
D_{SUYDAM}

Fig. 1

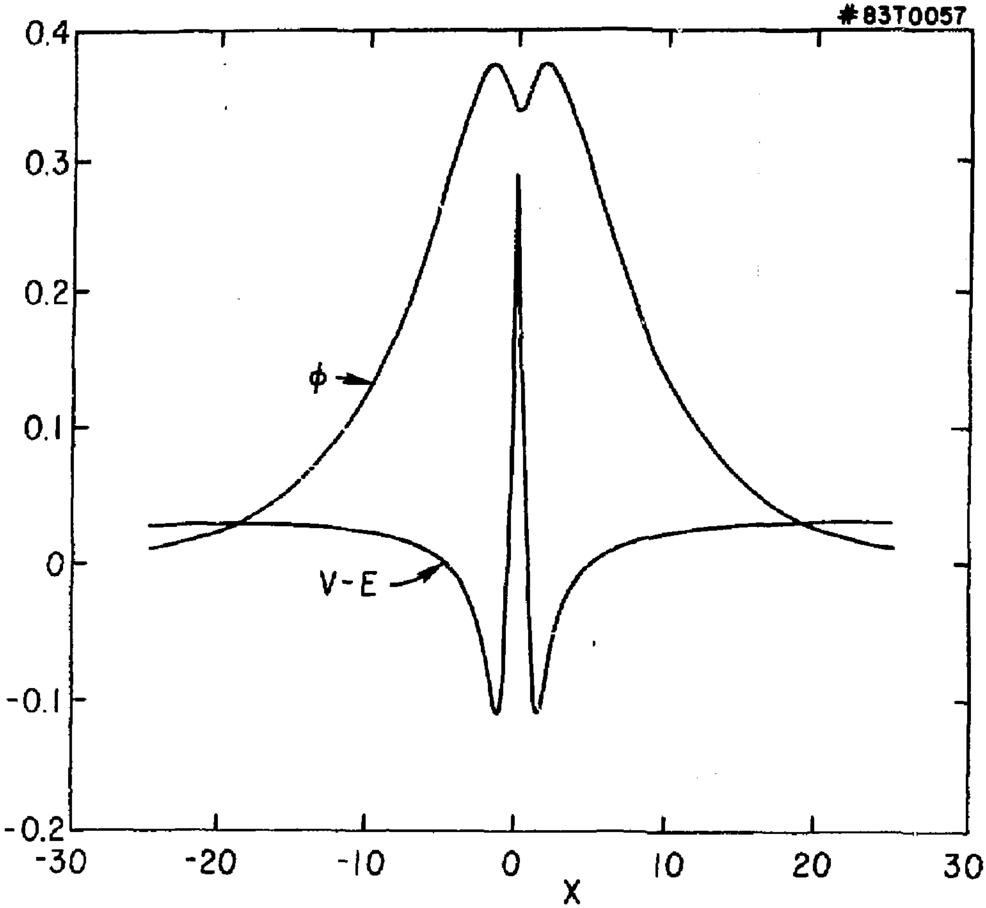

Fig. 2

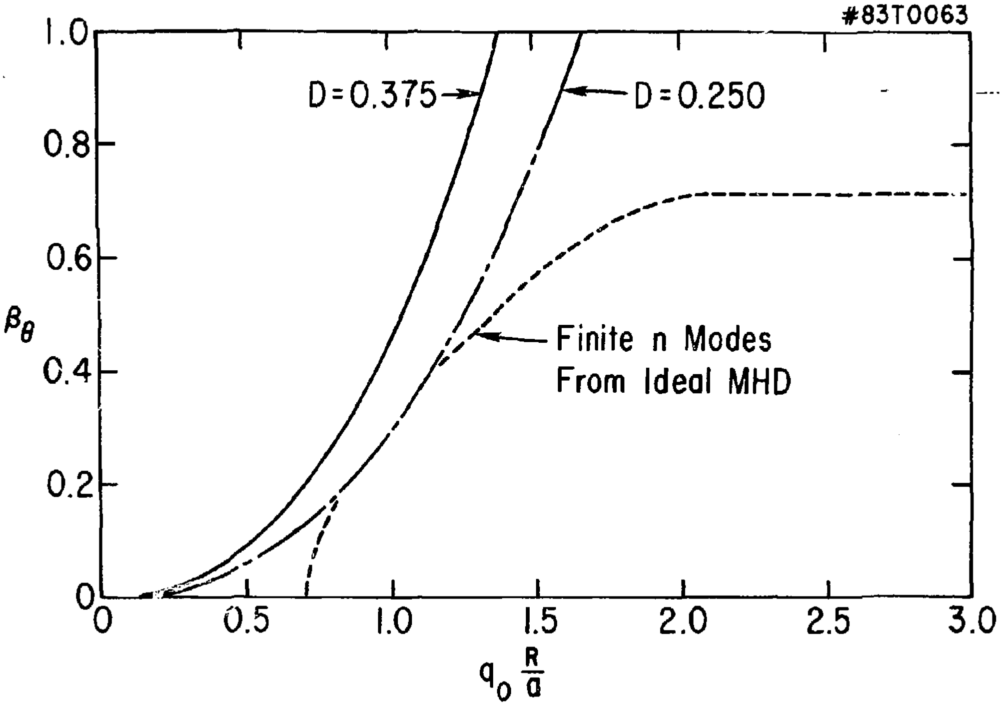
#83T0063
1.0
0.8
0.6
0.4
0.2
0
β_θ
D=0.375
D=0.250
Finite n Modes
From Ideal MHD
0
0.5
1.0
1.5
2.0
2.5
3.0
$q_0 \frac{R}{a}$

Fig. 3

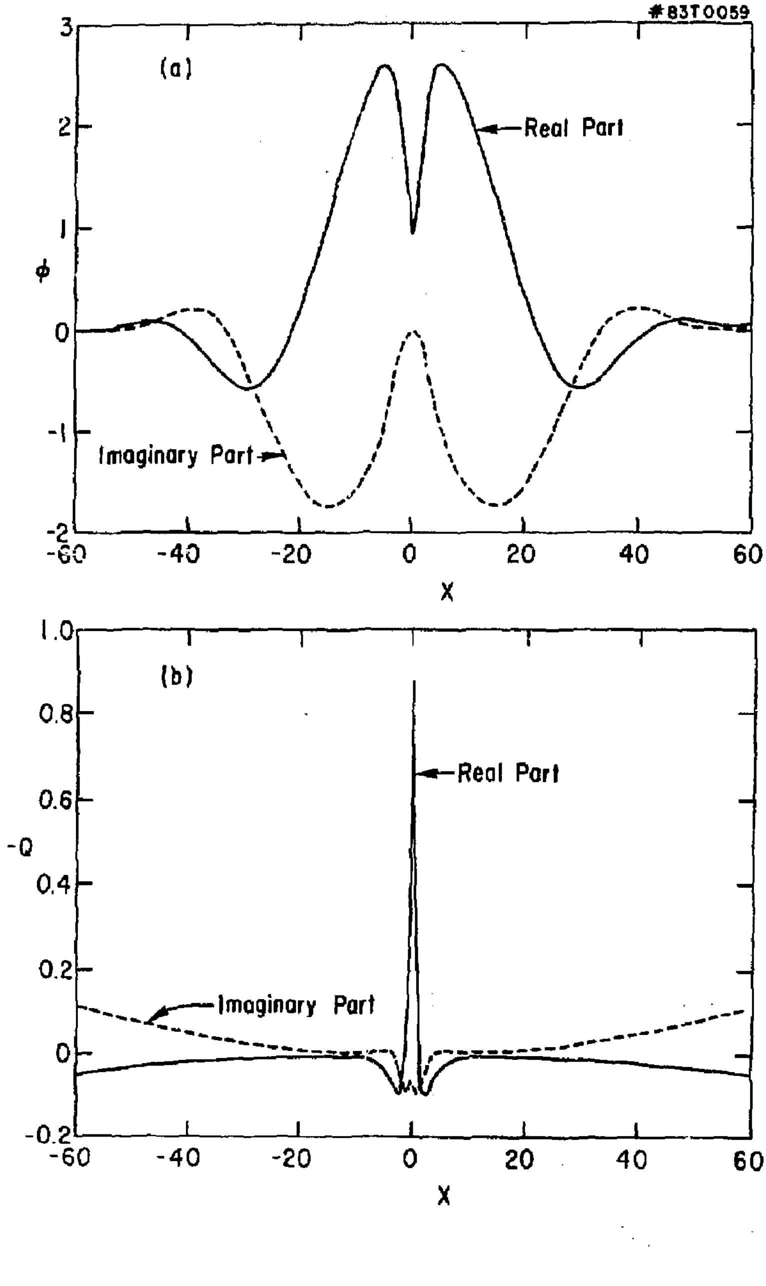
#83T0059
(a)
Real Part
Imaginary Part
φ
3
2
1
0
-1
-2
-60
-40
-20
0
20
40
60
X
(b)
Real Part
Imaginary Part
-Q
1.0
0.8
0.6
0.4
0.2
0
-0.2
-60
-40
-20
0
20
40
60
X

Fig. 4

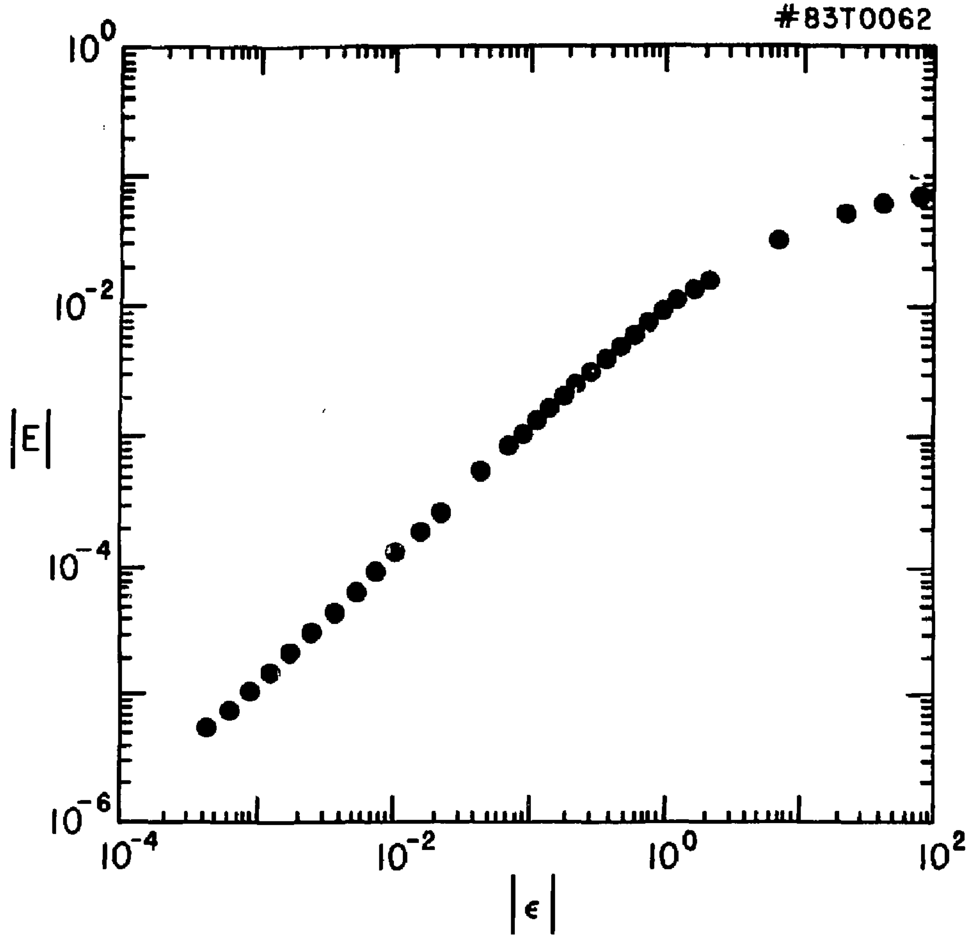

Fig. 5

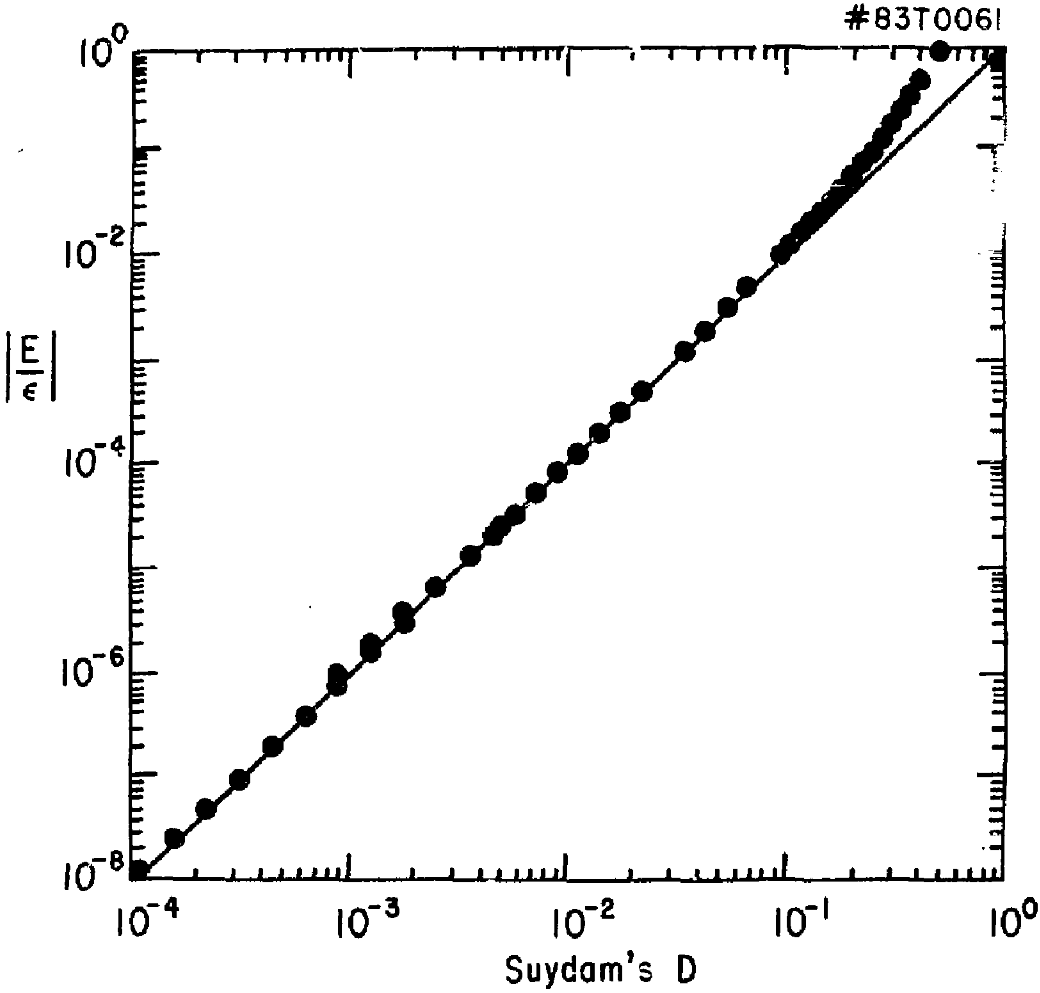
#83T0061
10^0
10^{-2}
10^{-4}
10^{-6}
10^{-8}
$\left|\frac{E}{\epsilon}\right|$
10^{-4}
10^{-3}
10^{-2}
10^{-1}
10^0
Suydam's D

Fig. 6

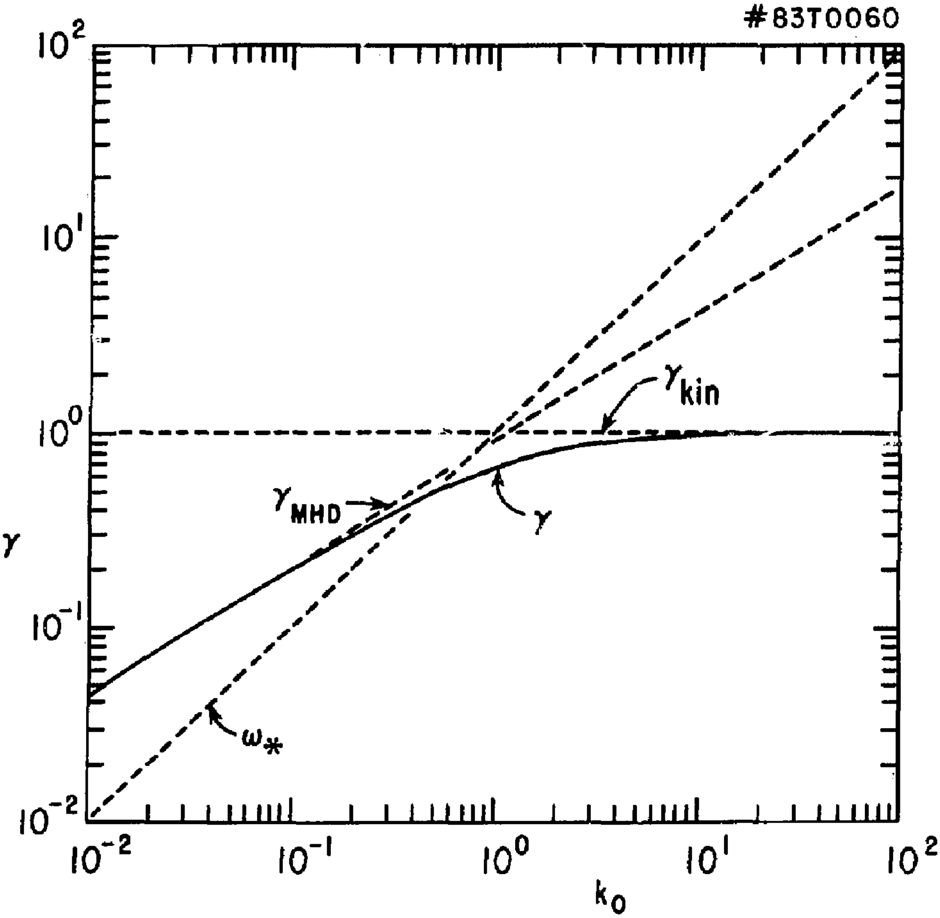
#83T0060
10^2
10^1
10^0
10^{-1}
10^{-2}
γ
γ_{kin}
γ_{MHD}
γ
ω_*
10^{-2}
10^{-1}
10^0
10^1
10^2
k_0

Fig. 7

EXTERNAL DISTRIBUTION IN ADDITION TO TIC UC-20

Plasma Res Lab, Austra Nat'l Univ, AUSTRALIA
Dr. Frank J. Paoloni, Univ of Wollongong, AUSTRALIA
Prof. I.R. Jones, Flinders Univ., AUSTRALIA
Prof. M.H. Brennan, Univ Sydney, AUSTRALIA
Prof. F. Cap, Inst Theo Phys, AUSTRIA
Prof. Frank Verheest, Inst theoretische, BELGIUM
Dr. D. Palumbo, Dg XII Fusion Prog, BELGIUM
Ecole Royale Militaire, Lab de Phys Plasmas, BELGIUM
Dr. P.H. Sakanaka, Univ Estadual, BRAZIL
Dr. C.R. James, Univ of Alberta, CANADA
Prof. J. Teichmann, Univ of Montreal, CANADA
Dr. H.M. Skarsgard, Univ of Saskatchewan, CANADA
Prof. S.R. Sreenivasan, University of Calgary, CANADA
Prof. Tudor W. Johnston, INRS-Energie, CANADA
Dr. Hannes Barnard, Univ British Columbia, CANADA
Dr. M.P. Bachynski, MPB Technologies, Inc., CANADA
Zhengwu Li, SW Inst Physics, CHINA
Library, Tsing Hua University, CHINA
Librarian, Institute of Physics, CHINA
Inst Plasma Phys, SW Inst Physics, CHINA
Dr. Peter Lukac, Komenskeho Univ, CZECHOSLOVAKIA
The Librarian, Culham Laboratory, ENGLAND
Prof. Schatzman, Observatoire de Nice, FRANCE
J. Radet, CEN-BP6, FRANCE
AM Dupas Library, AM Dupas Library, FRANCE
Dr. Tom Mual, Academy Bibliographic, HONG KONG
Preprint Library, Cent Res Inst Phys, HUNGARY
Dr. A.K. Sundaram, Physical Research Lab, INDIA
Dr. S.K. Trehan, Panjab University, INDIA
Dr. Indra, Mohan Lal Das, Banaras Hindu Univ, INDIA
Dr. L.K. Chavda, South Gujarat Univ, INDIA
Dr. R.K. Chhajlani, Var Ruchi Marg, INDIA
B. Buti, Physical Research Lab, INDIA
Dr. Phillip Rosenau, Israel Inst Tech, ISRAEL
Prof. S. Cuperman, Tel Aviv University, ISRAEL
Prof. G. Rostagni, Univ Di Padova, ITALY
Librarian, Int'l Ctr Theo Phys, ITALY
Miss Clelia De Palo, Assoc EURATOM-CNEN, ITALY
Biblioteca, del CNR EURATOM, ITALY
Dr. H. Yamato, Toshiba Res & Dev, JAPAN
Prof. M. Yoshikawa, JAERI, Tokai Res Est, JAPAN
Prof. T. Uchida, University of Tokyo, JAPAN
Research Info Center, Nagoya University, JAPAN
Prof. Kyoji Nishikawa, Univ of Hiroshima, JAPAN
Sigeru Mori, JAERI, JAPAN
Library, Kyoto University, JAPAN
Prof. Ichiro Kawakami, Nihon Univ, JAPAN
Prof. Satoshi Itoh, Kyushu University, JAPAN
Tech Info Division, Korea Atomic Energy, KOREA
Dr. R. England, Civdad Universitaria, MEXICO
Bibliotheek, Fom-Inst Voor Plasma, NETHERLANDS
Prof. B.S. Liley, University of Waikato, NEW ZEALAND
Dr. Suresh C. Sharma, Univ of Calabar, NIGERIA
Prof. J.A.C. Cabral, Inst Superior Tech, PORTUGAL
Dr. Octavian Petrus, ALI CUZA University, ROMANIA
Dr. R. Jones, Nat'l Univ Singapore, SINGAPORE
Prof. M.A. Hellberg, University of Natal, SO AFRICA
Dr. Johan de Villiers, Atomic Energy Bd, SO AFRICA
Dr. J.A. Tagle, JEN, SPAIN
Prof. Hans Wilhelmson, Chalmers Univ Tech, SWEDEN
Dr. Lennart Stenflo, University of UMEA, SWEDEN
Library, Royal Inst Tech, SWEDEN
Dr. Erik T. Karlson, Uppsala Universitet, SWEDEN
Centre de Recherchesen, Ecole Polytech Fed, SWITZERLAND
Dr. W.L. Weise, Nat'l Bur Stand, USA
Dr. W.M. Stacey, Georg Inst Tech, USA
Dr. S.T. Wu, Univ Alabama, USA
Mr. Norman L. Oleson, Univ S Florida, USA
Dr. Benjamin Ma, Iowa State Univ, USA
Magne Kristiansen, Texas Tech Univ, USA
Dr. Raymond Askew, Auburn Univ, USA
Dr. V.T. Tolok, Kharkov Phys Tech Ins, USSR
Dr. D.D. Ryutov, Siberian Acad Sci, USSR
Dr. M.S. Rabinovich, Lebedev Physical Inst, USSR
Dr. G.A. Eliseev, Kurchatov Institute, USSR
Dr. V.A. Glukhikh, Inst Electro-Physical, USSR
Prof. T.J. Boyd, Univ College N Wales, WALES
Dr. K. Schindler, Ruhr Universitat, W. GERMANY
Nuclear Res Estab, Julich Ltd, W. GERMANY
Librarian, Max-Planck Institut, W. GERMANY
Dr. H.J. Kaeppler, University Stuttgart, W. GERMANY
Bibliothek, Inst Plasmaforschung, W. GERMANY